



Improvement of the superconducting properties of carbon addition on $\text{Bi}_{1.6}\text{Pb}_{0.4}\text{Sr}_2\text{Ca}_2\text{Cu}_3\text{O}_{10+\delta}$ prepared through the two-step sintering process

Dini Rizqi Dwi Kunti SIREGAR¹, Sigit Dwi YUDANTO², Septian Adi CHANDRA², Eka Feby Ronauli LUBIS¹, Syahrul HUMAIDI¹, and Nono DARSONO^{2,*}

¹ Department of Physics, FMIPA, Universitas Sumatera Utara Jl. Bioteknologi No.1, Kampus USU, Medan 20155, Indonesia

² Research Center for Metallurgy and Materials, Indonesian Institute of Sciences, Gedung 470, South Tangerang, Banten, 15314, Indonesia

*Corresponding author e-mail: nono002@lipi.go.id

Received date:

27 June 2021

Revised date

7 September 2021

Accepted date:

7 September 2021

Keywords:

$\text{Bi}_{1.6}\text{Pb}_{0.4}\text{Sr}_2\text{Ca}_2\text{Cu}_3\text{O}_{10+\delta}$;
Sol-gel;
Carbon nanoparticles;
Carbon nanotubes;
Critical temperature

Abstract

The effects of the addition of carbon nanoparticles and nanotubes on the $\text{Bi}_{1.6}\text{Pb}_{0.4}\text{Sr}_2\text{Ca}_2\text{Cu}_3\text{O}_{10+\delta}$ (BPSCCO) have been reported. BPSCCO samples were synthesized using the sol-gel method. BPSCCO with nominal composition was sintered at 840°C for 30 h, then grounded and added an amount of carbon. Pure and carbon added BPSCCO were sintered at 840°C for 30 hours. Resistivity measurements were carried out to determine the superconducting properties of the samples. We found that the addition of carbon nanoparticles and nanotubes increased the critical zero temperature ($T_{c\text{-zero}}$) of BPSCCO from 94.67 K to 97.8 K and 102.03 K for the pure BPSCCO, 0.05 wt% carbon nanoparticles added BPSCCO, and 0.2 wt% carbon nanotubes added BPSCCO, respectively. Based on the X-ray diffraction and SEM results, we can see that the main phase formed in the samples is dominated by the orthorhombic Bi-2212 phase structure, and the morphology typical of the BPSCCO superconductor which is a plate-like granular form has been observed in all samples.

1. Introduction

A new era in superconductivity studies began in 1986 with the discovery of high-temperature superconducting (HTS). Bismuth strontium calcium copper oxide known as BSCCO is the next high-temperature member of the HTS family. The BSCCO system, $\text{Bi}_2\text{Sr}_2\text{Ca}_{n-1}\text{Cu}_n\text{O}_{2n+4+\delta}$ ($n = 1, 2, 3$), has a critical temperature value of 20 K ($n=1$) denoted as Bi-2201, 85 K ($n=2$) denoted as Bi-2212, and 110 K ($n=3$) denoted as Bi-2223 [1]. The only difference between the two successive phases is that the double Ca-Cu-O is added to the unit cell [2,3]. Among the three phases, 2223 phase is the most promising phase for high current applications like cables, power cables [4], generators [5], transformers [6], motors [7], and fault current limiters [8]. However, the main problem in Bi-based superconductor is weak inter-grain connectivity [9]. To solve it, one of the most useful techniques, in this regard, is the substitution of some elements at different cationic sites [10]. Doping with Pb in the Bi site has been studied in several works showing that the presence of Pb enhances the connections between grains [11].

Safran *et al.* synthesized the $\text{Bi}_{1.85}\text{Pb}_{0.35}\text{Sr}_2\text{Ca}_2\text{Cu}_3\text{O}_{10+\delta}$ using the re-pelletized and re-sintering method [12]. They reported that it is known that denser and harder materials were formed with re-granulation by bridging the interstices between the grains. Repeated sintering increases grain size and enhances T_c effectiveness. Thus, it can increase the critical temperature and have a positive effect on the critical current density value of the sample [12]

Darsono *et al.* reported that the optimal heating temperature for the evolution of microstructure and phase structure is at a temperature of 840°C, where the sample was prepared by the citrate-based sol-gel method using the appropriate nitrate as the starting material [13]. The sol-gel method is a method that can be used to synthesize the BPSCCO material. Samples synthesized by using liquid-phase combustion have a smaller chance of impurities than synthesis in the solid state. In addition, the advantage of the sol-gel method over all other synthetic routes it provides better homogeneity, better control of particle size, and requires a shorter heat treatment [14-16]

Many reports show that the high-temperature superconductor BSCCO, doped by carbon nanoparticles and nanotubes (CNTs), effectively improves the superconductivity properties [17-21]. The critical current density (J_c) was improved due to very good grain connectivity, although decreasing the critical temperature [19]. It has previously been shown by Galvan *et al.* [18] and Ozcelik *et al.* [21] that it is possible to doped nanotubes inside a BSCCO superconductor with a subsequent enhancement in the inter-grain critical current density, due to the fact that carbon nanotubes have a shape and size similar to that of columnar defects induced in BSCCO. It can act as center brace flux because of their small size. Saoudeh *et al.* added carbon nanotubes to commercial BPSCCO. They reported that CNTs addition improves the microstructure and increases the grain size and grain connectivity. The disadvantages of the addition CNT on the BPSCCO was decreased of the critical temperature and the volume fraction of the Bi-2223 phase [20].

In this study, we investigate the influence of the carbon nanoparticles and nanotubes addition on the superconducting properties of BPSCCO. The pure and carbon added BPSCCO was prepared using a sol-gel method followed by the two-step sintering process. The cryogenic magnetometer was used for the evaluation of the superconducting properties of all samples.

2. Experimental

2.1 Materials and procedures

The pure and carbon added BPSCCO samples were prepared using the sol-gel method followed by the two-step sintering process. Carbon nanoparticles (from Sigma Aldrich Chemicals with a purity >99% and <100 nm particle size) and carbon nanotube (Multi-Walled Carbon Nanotube (MWCNT) from Sigma Aldrich Chemicals with 8 μm to 10 μm length powder and >97% purity) as dopant of BPSCCO sample. The bismuth nitrate, lead nitrate, strontium nitrate, calcium nitrate, and copper nitrate (all from Sigma Aldrich Chemicals with a purity >99%) as raw materials were weighed stoichiometry at the nominal composition of Bi:Pb:Sr:Ca:Cu = 1.6:0.4:2:2:3 and dissolved in the distilled water separately. All solutions were mixed, and the citric acid was added to the mixed solution with the metal to citric acid ratio of 1:1.2. In the previous work, ethylene glycol was added as a complexing agent [13]. Furthermore, the absence of ethylene glycol will be studied for the formation of the Bi-2223 phase. The ammonia solution was wisely dropped to get a neutral solution (pH = ~7). Subsequently, the neutral solution was heated at 80°C to 110°C while stirring to produce a dark green gel. During the heating, the gel was exothermically burned, resulting in black and dry powder. The decomposed powder was then heated at 300°C and 500°C. The resulting powder was manually ground and calcined at 800°C for 6 h. Finally, the powder was compacted into cylindrical-pellets with diameter of 10 mm and thickness of 3 mm, it was sintered at 840°C (first step sintering). The samples were kept in the furnace for 30 h and cooled naturally. After sintering, one pellet was characterized (B-S1). Four samples were prepared for the second sintering: pure BPSCCO (B-S2), 0.2 wt% carbon nanotubes (B-C1), 0.05 wt% carbon nanoparticles (B-N1) and 0.2 wt% carbon nanoparticles (B-N2) added BPSCCO. For the carbon added BPSCCO sample, an amount of carbon was mixed with the powder obtained by the first step sintering process and ground using an agate mortar. The powder was then compacted into pellets and sintered at a temperature of 840°C for 30 h (second step sintering process).

2.2 Material characterization

The phase compound and surface morphology of the samples were examined by means X-ray diffraction (XRD) with the $\text{Co-K}\alpha$ radiation source ($\lambda = 1.7903 \text{ \AA}$) and Scanning Electron Microscopy (SEM), respectively. The resistivity of the samples was measured using a cryogenic magnetometer with the four-point probe method to evaluate the superconducting properties.

3. Results and discussion

After sintering, the bulk sample was ground and characterized using an XRD. Figure 1 shows the diffraction patterns of the pure and carbon added BPSCCO prepared by two-step sintering process. Bi-2212 and Bi-2223 phase with orthorhombic and tetragonal structures was detected in the BPSCCO sample as major phase. Several phases, like CuO, Ca_2PbO_4 , CaCu_2O_3 , and Sr_2CuO_3 phase were also found as minor phase. This result is not significantly different from the previous results [13]. Imperfect reaction and decomposition during the sintering process led to the formation of Ca_2PbO_4 and CuO phases. The CaO and Pb-rich liquid reaction initiates the Ca_2PbO_4 phase, and the CaCu_2O_3 phase is formed by the reaction of CaO and CuO [22,23].

Based on the XRD results for the sample (B-S2), it shows that the second step sintering process can improve the Bi-2223 phase formation reaction. It can be seen clearly decreasing the peak intensity of Ca_2PbO_4 and Sr_2CuO_3 phase at an angle of $2\theta = 20.72^\circ$ and $2\theta = 32.7^\circ$. The minor phase CaCu_2O_3 was also disappeared in the second step sintering process.

A quantitative analysis was performed to estimate the volume fraction of the Bi-2223 phase formed. The volume fractions of the Bi-2223 (H) and Bi-2212 (L) phases were calculated based on the sum of the integrated peak intensities [22] for the pure and carbon added BPSCCO samples, as summarized in Table 1. Bi-2223 phase in pure BPSCCO sample with the first step sintering process (B-S1) increased from 22.00% to 24.94% compared by the second step sintering process (B-S2). The highest Bi-2223 phase of 27.89% was obtained by adding 0.2 wt% carbon nanotube. Thus, the second step sintering process promotes the formation of the Bi-2223 phase [24].

To obtain lattice parameters of the sample we calculate by the least square method and used h, k, l as the Miller indices and d as the interplanar distances [25]. The crystal structure of pure BPSCCO samples with two-step sintering indicates the dominant phase formed is Bi-2212 with orthorhombic phases with the lattice parameters $a = 5.409 \text{ \AA}$, $b = 5.386 \text{ \AA}$ and $c = 30.80 \text{ \AA}$. The addition of carbon nanoparticles and nanotubes does not change the crystal structure and lattice parameters, it is shown in Table 2.

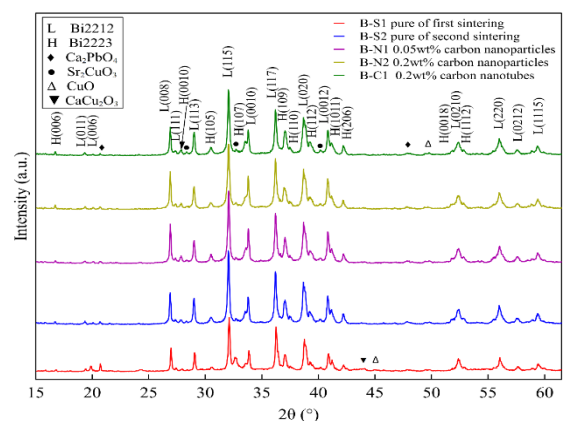


Figure 1 Diffraction patterns of the pure and carbon added BPSCCO sample prepared by two-step sintering process.

Table 1. Quantitative analysis of XRD data.

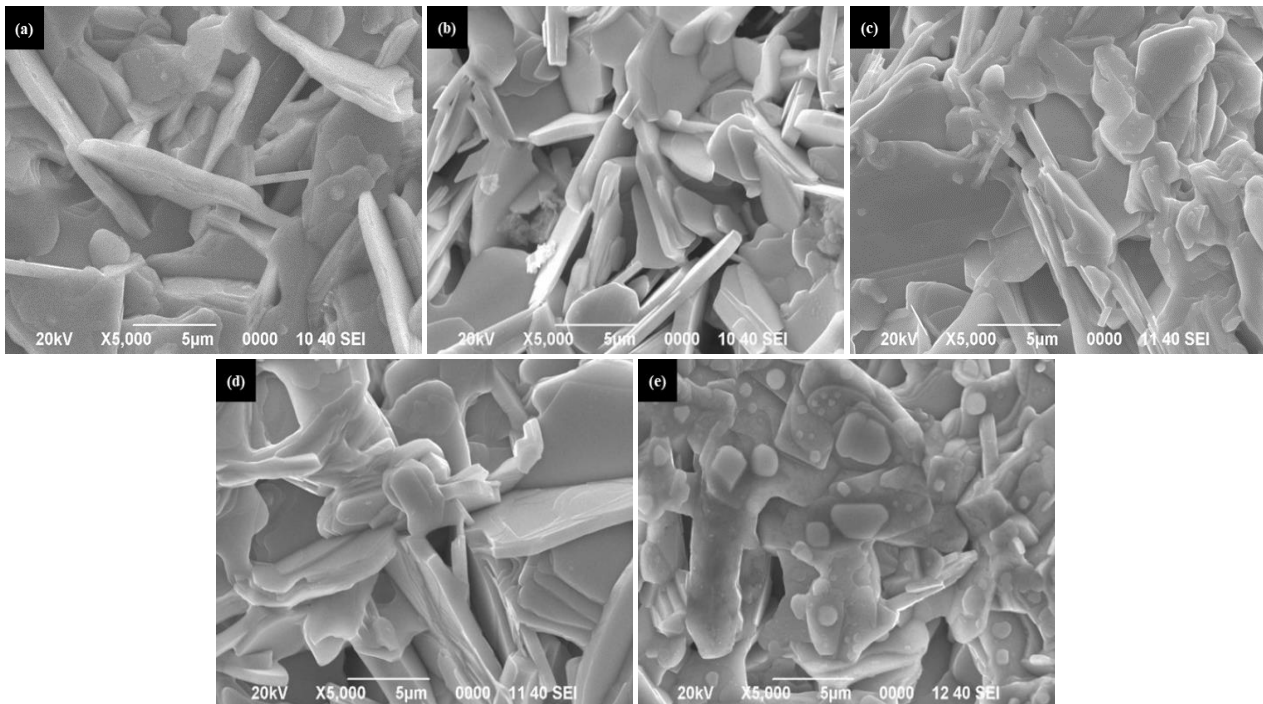
Sample code	Note	Bi-2212	Bi-2232	Bi-2223 crystallite size
		(vol. phase, %)	(vol. phase, %)	(nm)
B-S1	Pure of first sintering	78.00	22.00	105
B-S2	Pure of second sintering	75.06	24.94	61
B-N1	0.05 wt% carbon nanoparticles	73.41	26.59	51
B-N2	0.2 wt% carbon nanoparticles	76.72	23.28	43
B-C1	0.2 wt% CNT	72.11	27.89	52

Table 2. The lattice parameters (a, b, and c) of Bi-2212 and Bi-2223 phase for all samples.

Sample code	Note	Lattice parameters					
		(Bi-2212 phase)			(Bi-2223 phase)		
		a (Å)	b (Å)	c (Å)	a (Å)	b (Å)	c (Å)
B-S1	Pure of first sintering	5.390	5.378	30.74	3.937	3.937	37.08
B-S2	Pure of second sintering	5.409	5.386	30.80	3.939	3.939	37.20
B-N1	0.05 wt% carbon nanoparticles	5.407	5.378	30.78	3.940	3.940	37.19
B-N2	0.2 wt% carbon nanoparticles	5.403	5.383	30.79	3.934	3.934	37.18
B-C1	0.2 wt% CNT	5.402	5.383	30.79	3.940	3.940	37.19

Figure 2 shows an SEM image of the pure and carbon added BPSSCO samples. It can be seen that the typical morphology of the superconductor BSCCO was seen in the pure BPSSCO sample (B-S1) [13,26]. In the B-S2 sample, it looks the fine and dense grains compared with the B-S1 sample. This shows that the sol-gel method followed by the two-step sintering process can improve the grain connectivity and refine the grain size. The addition of 0.2 wt% carbon nanotubes has a better grain orientation and looks more evenly distributed to one another and the space between the plates (voids) is relatively less so that the porosity formed is smaller than the pure sample. During the sintering process, crystal diffusion across the grain boundaries occurs and an expansion of the contact area between

crystals will increase the grain size and the recrystallization process and grain growth occur [27]. In Figure 2, it can be seen that the addition of carbon nanoparticles and carbon nanotubes increasing the grain size of the sample as reported by Saoudel *et al.* [20]. As shown in Figures 2(a) and 2(b), the grain sizes vary between 0.1 μm and 0.3 μm for the pure samples, grain size for sample B-N1 and B-N2 increases between 0.3 μm and 0.5 μm (see Figures 2(c) and 2(d)). The grain size shape for sample B-C1 is formed by small grains smaller than 0.1 μm , and the others are rectangular plates that are much larger than the others ($>0.5 \mu\text{m}$) (see Figure 2(e)). Larger grain sizes and well-connected grains are required to obtain better superconducting parameters [12].

**Figure 2.** SEM images of the pure and carbon added BPSSCO samples (a) pure of first sintering, (b) pure of second sintering, (c) 0.05 wt% carbon nanoparticles, (d) 0.2 wt% carbon nanoparticles, and (e) 0.2 wt% carbon nanotubes added BPSSCO.

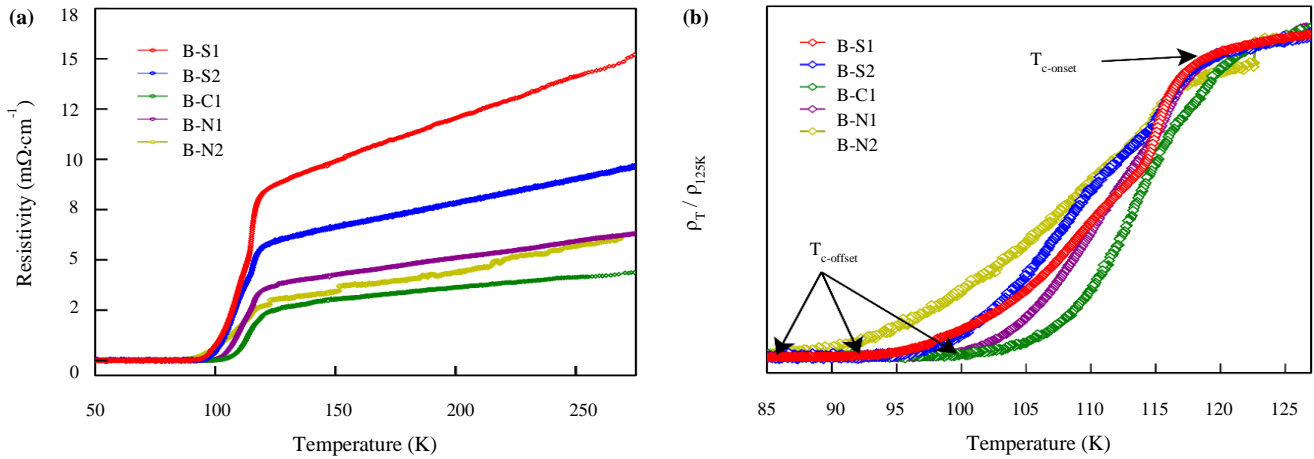


Figure 3. Electrical resistivity of the pure and carbon added BPSCCO samples (a) R-T curve, and (b) normalized resistivity vs temperature.

Table 3. Electrical resistivity and the critical temperature of B-S1, B-S2, B-N1, B-N2 and B-C2.

Sample code	ρ at 270 K ($\text{m}\Omega\cdot\text{cm}$)	ρ at 125 K ($\text{m}\Omega\cdot\text{cm}$)	$T_{\text{c-onset}}$ (K)	$T_{\text{c-offset}}$ (K)	ΔT_{c} (K)
B-S1	14.87	8.73	117.5	91.46	26.04
B-S2	9.54	5.95	117.62	94.67	22.95
B-N1	6.24	3.70	118.35	97.8	20.55
B-N2	6.05	3.03	117.6	89.18	28.42
B-C1	4.34	2.51	119.43	102.03	17.4

To evaluate the superconducting properties of the samples, we measure the electrical resistance of the samples using a cryogenic magnetometer with the four-point probe (FPP) method. Figure 3(a) shows the electrical resistivity versus temperature for the pure and carbon added BPSCCO samples. The deviation from the linear behavior of about 117 K to 119 K has been considered as the critical onset temperature ($T_{\text{c-onset}}$). These values have been determined from the resistivity versus temperature curve. Table 3 shows the electrical resistivity and superconducting properties of all samples. The electrical resistivity of the samples is below zero in the range 102 K to 91 K, the critical zero temperature ($T_{\text{c-offset}}$). As can be seen clearly in Figure 3(b), there has been a sharp superconductor transition under $T_{\text{c-onset}}$ for all samples. There is a large critical temperature gap (ΔT_{c}) value, this indicates that the Bi-2212 phase is the more dominant one for all samples.

The two-step sintering process and addition of carbon in the BPSCCO decreased the electrical resistivity value of the sample. Overall, the 0.2 wt% carbon nanotubes added BPSCCO sample shows the highest T_{c} value. The small increase in $T_{\text{c-offset}}$ compared to pure BPSCCO samples can be explained by the better grain orientation and stronger inter-grain links when examined by SEM results of all samples. On the other hand, the addition of 0.05 wt% carbon nanoparticles results in a higher T_{c} value when compared to the addition of 0.2 wt% carbon nanoparticles, which means that the smaller the percentage of the additional weight of carbon nanoparticles will increase the critical temperature of the BPSCCO sample. However, the addition of carbon nanoparticles results in a relatively lower T_{c} value when it is compared to the addition of 0.2 wt% carbon nanotubes samples which may be due to significant defects. This presence can be detected based on the ΔT_{c} . As shown in Table 3, the ΔT_{c} in

the sample is inversely proportional to the resulting critical temperature for all samples. The smaller the critical temperature gap of the sample, the higher the T_{c} value. In general, the ranges of $T_{\text{c-onset}}$ and $T_{\text{c-offset}}$ values of all samples are not very close. The value of the ΔT_{c} obtained is still high. This can also be attributed to the decomposition of the Bi-2223 phase to the Bi-2212 phase.

4. Conclusions

In this study, we have synthesized the pure and carbon added BPSCCO by the sol-gel method followed by a two-step sintering process. The second step sintering process and the addition of carbon nanoparticles and carbon nanotubes improve the Bi-2223 phase formation, refined grain size, grain connectivity, and the critical temperature. The addition of doping of 0.05 wt% carbon nanoparticles and 0.2 wt% carbon nanotubes can increase the critical temperature value and the volume fraction of Bi-2223. It is found that the highest critical temperature value in the 0.2 wt% carbon nanotubes added BPSCCO with $T_{\text{c-offset}}$ of 102.03 K and an increase in the value of the Bi-2223 phase volume, is the best result when compared to other samples. Carbon nanotubes behaves more effectively than carbon nanoparticles in the BPSCCO compound to improve its properties.

Acknowledgements

The authors would like to thank the Research Center for Metallurgy and Materials for the support of the research facilities. This work was funded by the National Research and Innovation Agency of the Republic of Indonesia.

References

- [1] A. K. Jassim, "Improvement of superconducting parameters of $\text{Bi}_{1.6}\text{Pb}_{0.4}\text{Sr}_2\text{Ca}_2\text{Cu}_3\text{O}_{10+\delta}$ added with Au nanoparticles," *Iraqi Journal of Physics*, vol. 16, no. 38, pp. 99-111, 2018.
- [2] C. P. Poole, H. A. Farach, and R. J. Creswick, *Superconductivity*, Second. Netherlands: Elsevier, 2007.
- [3] Y-F. Lv, W-L. Wang, J-P. Peng, H. Ding, Y. Wang, L. Wang, K. He, S-H. Ji, R. Zhong, J. Schneeloch, G-D. Gu, C-L. Song, X-C. Ma, and Q-K. Xue, "Mapping the electronic structure of each ingredient oxide layer of high-Tc cuprate superconductor $\text{Bi}_2\text{Sr}_2\text{CaCu}_2\text{O}_{8+\delta}$," *Physical Review Letters*, vol. 115, no. 23, pp. 1-5, 2015.
- [4] O. V. Kharissova, E. M. Kopnin, V. V. Maltsev, N. I. Leonyuk, L. M. Leon-Rossano, I. Yu. Pinus, and B. I. Kharisov, "Recent advances on bismuth-based 2223 and 2212 superconductors: Synthesis, chemical properties, and principal applications," *Critical Reviews in Solid State and Materials Sciences*, vol. 39, no. 4, pp. 253-276, 2014.
- [5] W. Stautner, R. Fair, K. Sivasubramaniam, K. Amm, J. Bray, E. T. Laskaris, K. Weeber, M. Douglass, L. Fulton, S. Hou, J-Ho. Kim, R. Longtin, M. Moscinski, J. Rochford, R. Rajput-Ghoshal, P. Riley, D. J. Wagner, and R. Duckworth, "Large scale superconducting wind turbine cooling," *IEEE Transaction on Applied Superconductivity*, vol. 23, no. 3, pp. 5200804-5200804, 2013.
- [6] J. X. Jin, Y. J. Tang, X. Y. Xiao, B. X. Du, Q. L. Wang, J. H. Wang, S. H. Wang, Y. F. Bi, and J. G. Zhu, "HTS Power devices and systems : Principles, characteristics, performance, and efficiency," *IEEE Transaction on Applied Superconductivity*, vol. 26, no. 7, pp. 1-26, 2016.
- [7] Y. Koshihara, S. Yuan, N. Maki, M. Izumi, K. Umemoto, K. Aizawa, Y. Kimura, and M. Yokoyama, "Critical current and electric loss under magnetic field at 30 K on Bi-2223 superconducting coil for ship propulsion motor," *IEEE Transaction on Applied Superconductivity*, vol. 21, no. 3, pp. 1127-1130, 2011.
- [8] N. Yonemura, K. Yamabe, Y. Shirai, S. Kobayashi, T. Nagaishi, and M. Konishi, "Current limiting performance of transformer-type superconducting fault current limiter made of BSCCO and REBCO wires," *IEEE Transaction on Applied Superconductivity*, vol. 25, no. 3, pp. 1-4, 2015.
- [9] S. Safran, A. Kılıç, and O. Ozturk, "Effect of re-pelletization on structural , mechanical and superconducting properties of BSCCO superconductors," *Journal of Materials Science: Materials in Electronics*, vol. 28, no. 2, pp. 1799-1803, 2016.
- [10] B. Özçelik, M. Gürsul, A. Sotelo, and M. A. Madre, "Improvement of superconducting properties in Na-doped BSCCO superconductor," *Journal of Materials Science: Materials in Electronics*, vol. 26, no. 1, pp. 441-447, 2015.
- [11] A. Biju, P. Guruswamy, and U. Syamaprasad, "Influence of Pb on structural and superconducting properties of rare earth modified $\text{Bi}_2\text{Sr}_2\text{CaCu}_2\text{O}_y$," vol. 466, no. 1-2, pp. 23-28, 2007.
- [12] S. Safran, H. Ozturk, F. Bulut, and O. Ozturk, "The influence of re-pelletization and heat treatment on physical, superconducting, magnetic and micro-mechanical properties of bulk BSCCO samples prepared by ammonium nitrate precipitation method," *Ceramics International*, vol. 43, no. 17, pp. 15586-15592, 2017.
- [13] N. Darsono, and D. Y. K. Raju, "Effects of the Sintering conditions on the structural phase evolution and T C of $\text{Bi}_{1.6}\text{Pb}_{0.4}\text{Sr}_2\text{Ca}_2\text{Cu}_3\text{O}_7$ prepared using the citrate sol-gel method," *Journal of Superconductivity and Novel Magnetism*, vol. 29, no. 6, pp. 1491-1497, 2016.
- [14] V. D. Rodrigues, G. A. De Souza, C. L. Carvalho, R. Zadorosny, F. De Engenharia, and I. Solteira, "Effect of La doping on the crystal structure, electric, magnetic and morphologic properties of the BSCCO system 2. material and experimental procedure," *Materials Research*, vol. 20, no. 5, pp. 1406-1413, 2017.
- [15] M. Shamsodini, H. Salamati, H. Shakeripour, I. A. Sarsari, M. F. Esferize, and H. Nikmanesh, "Effect of using two different starting materials (Nitrates and Carbonates) and calcination process on the grain boundaries properties of BSCCO superconductor," *Superconductor Science and Technology*, vol. 32, no. 7, p. 075001, 2019.
- [16] A. Coşkun, G. Akça, E. Taşarkuyu, ö. Battal, and A. Ekicibil, "Structural, magnetic, and electrical properties of $\text{Bi}_{1.6}\text{Pb}_{0.4}\text{Sr}_2\text{Ca}_2\text{Cu}_3\text{O}_{10+x}$ superconductor prepared by different techniques," *Journal of Superconductivity and Novel Magnetism*, vol. 33, pp. 3377-3393, 2020.
- [17] D. H. Galvan, S. Li, W. M. Yuhasz, J. H. Kim, M. B. Maple, and E. Adem, "Nondestructive interactions of carbon nanotubes with $\text{Bi}_2\text{Sr}_2\text{CaCu}_2\text{O}_8$," *Physica C: Superconductivity*, vol. 403, no. 3, pp. 145-150, 2004.
- [18] D. H. Galvan, A. Duran, F. Castillon, E. Adem, R. Escudero, D. Ferere, A. Torres, and M. J. Yacaman, "Enhancement of the current density J C for $\text{Bi}_2\text{Sr}_2\text{CaCu}_2\text{O}_8$ by means of carbon and NbSe 2 nanotubes," *Journal of Superconductivity and Novel Magnetism*, vol. 21, no. 5, pp. 271-277, 2008.
- [19] A. Saoudeh, A. Amira, Y. Boudjadja, L. Amirouche, N. Mahamdioua, A. Varilci, S. P. Altintas, and C. Terzioglu, "On the effect of carbon nano-tubes addition on structure and superconducting properties of Bi(Pb)-2223 phase," *Journal of Superconductivity and Novel Magnetism*, vol. 26, no. 4, pp. 861-865, 2012.
- [20] A. Saoudeh, A. Amira, Y. Boudjadja, N. Mahamdioua, L. Amirouche, and A. Varilci, "Study of the thermo-magnetic fluctuations in carbon nanotubes added Bi-2223 superconductors," *Physica B: Physics of Condensed Matter*, vol. 429, pp. 33-37, 2013.
- [21] B. Özçelik, I. Ergin, T. Depçi, H. I. Yavuz, M. A. Madre, and A. Sotelo, "Effect of carbon nanotube addition on the superconducting properties of BSCCO Samples textured via laser floating zone technique," *Journal of Superconductivity and Novel Magnetism*, vol. 32, pp. 3135-3141, 2019.
- [22] N. Darsono, A. Imaduddin, K. Raju, and D. H. Yoon, "Synthesis and characterization of $\text{Bi}_{1.6}\text{Pb}_{0.4}\text{Sr}_2\text{Ca}_2\text{Cu}_3\text{O}_7$ superconducting oxide by high-energy milling," *Journal of Superconductivity and Novel Magnetism*, vol. 28, no. 8, pp. 2259-2266, 2015.
- [23] H. Fallah-arani, S. Baghshahi, D. Stornaiuolo, F. Tafuri, D. Massarotti, and N. Riahi-noori, "The influence of heat treatment

- on the microstructure, flux pinning and magnetic properties of bulk BSCCO samples prepared by sol-gel route,” *Ceramics International*, vol. 44, no. 5, pp. 5209-5218, 2018.
- [24] I. Hamadneh, S. A. Halim, and C. K. Lee, “Characterization of $\text{Bi}_{1.6}\text{Pb}_{0.4}\text{Sr}_2\text{Ca}_2\text{Cu}_3\text{O}_y$ ceramic superconductor prepared via coprecipitation method at different sintering time,” *Journal of Materials Science*, vol. 41, no. 17, pp. 5526-5530, 2006.
- [25] T. Çördük, Ö. Bilgili, and K. Kocabaş, “Investigation of effects of MgO nanoparticles addition on the superconducting properties of Bi-2223 superconductors,” *Journal of Materials Science: Materials in Electronics*, vol. 28, no. 19, pp. 14689-14695, 2017.
- [26] S. M. Khalil, “Enhancement of superconducting and mechanical properties in BSCCO with Pb additions,” *Journal of Physics and Chemistry of Solids*, vol. 62, no. 3, pp. 457-466, 2001.
- [27] B. R. Lehnorff, *High - T_c Superconductors for Magnet and Energy Technology*. Springer Tracts in Modern Physics, 2001.